EXTENDED EXPERIMENTAL PROCEDURES

Tissue Processing, Flow Cytometry, and Cell Sorting

Microglia were sorted from mice after PBS perfusion and enzymatic digestion in HBSS containing collagenase D (Sigma, 1mg/ml), for 30 min at 37°C and then separated by 40% percoll-gradient centrifugation. Kupffer cells were sorted from mice perfused with PBS, subject to digestion in PBS containing 5% FBS, and 1mg/ml Collagenase VIII (Sigma), shaking for 45 min at 37°C, and supernatant was collected from three rounds of low speed centrifugation. Spleen red pulp macrophages and lung macrophages were sorted after enzymatic digestion in Collagenase IV (Sigma) at 37°C and RBC lysis for 1 min. Peritoneal cavity macrophages were isolated by lavage with PBS containing 2mM EDTA and 1% FBS. Intestinal macrophages were isolated as previously described (Zigmond et al., 2012), subject to epithelial segregation for 40 min in HBSS with 2 mM EDTA, and 1 mM DTT (Sigma) at 37°C, shaking and then digested in PBS containing 1mg/ml Collagenase VIII (Sigma), shaking for 40 min. Monocytes and neutrophils were isolated from bone marrow and separated on a ficoll density gradient. Cells were stained with Live/Dead fixable dead cell stain (Life technologies) prior to antibody staining. For cross-linking, cells were resuspended in RPMI containing 10% FBS and 1% formaldehyde for 10 min at RT, quenched in 2.5M glycine for 5 min, and washed three times in PBS, prior to sorting. The following antibodies were used for cell isolation: F4/80(CI:A3-1) (Serotec), CD11b (M1/70), CD45 (30-f11), CD45.2 (104), CD45.1 (A20), IAb (AF6-120.1), CD64 (X54-5/7.1), Ly6c (hk1.4), CD11c (N418), CD115 (AFS98), Ly6g (1A8), CD117 (2B8), NK1.1(pk136), TCRb (h57-597), B220 (ra3-6b2), Gr-1 (RB6-865), F4/80 (BM8), Icam2 (3C4) (all Biolegend), CD103 (m290), SiglecF (e50-2440) (BD Pharmigen). See also Data S1.

RNA Isolation

10^4-10^5 cells from each macrophage subpopulation were sorted in 100-200 μl of Lysis/Binding Buffer (Life technologies) with 1% β-mercaptoethanol, lysed for 5 min and frozen at −80°C. Cell lysates were thawed and mRNA was captured with 12 μl of Dynabeads oligo(dT) (Life technologies), and washed according to manufacture guidelines. Purified messenger RNA was eluted at 70°C with 10 μl of 10 mM Tris-Cl pH 7.5 and stored at −80°C.

RNA-Seq: Linear Amplification of mRNA

In brief, MARS-seq consists of special designed primers with unique molecular identifiers for accurate molecule counting and a step of linear amplification of the initial mRNA pool, followed by a library construction step. This preserves the diversity of the original pool of messenger RNAs, even if the amount of input RNA is low.

cDNA was generated from 1ul of mRNA of each sample. cDNA quantity in each sample was evaluated by qPCR for Actin B gene, and then equivalent amounts of mRNA of each sample were taken for RNaseq library construction. Library construction was performed in a 96-well plate format. First, to open secondary RNA structures and allow annealing of the RT primer, the samples were incubated at 72°C for 3 min and immediately transferred to 4°C. Then, RT reaction mix (10 mM DTT, 4 mM dNTP, 2.5 U/μl Superscript III RT enzyme in 50 mM Tris-HCl (pH 8.3), 75 mM KCl, 3 mM $MgCl_2$) was added into each well of the 96-well plate and the reaction was mixed. The 96-well plate was then spun down and moved into a cycler (Eppendorf) for the following incubation: 2 min at 42°C, 50 min at 50°C, 5 min at 85°C. Indexed samples with equivalent amount of cDNA were pooled. The pooled cDNA was converted to double-stranded DNA with a second strand synthesis kit (NEB) in a 20μl reaction, incubating for 2.5 hr at 16°C. The product was purified with 1.4x volumes of SPRI beads, eluted in 8 μl and in-vitro transcribed (with the beads) at 37°C overnight for linear amplification using the T7 High Yield RNA polymerase IVT kit (NEB). Following IVT, the DNA template was removed with Turbo DNase I (Ambion) 15 min at 37°C and the amplified RNA (aRNA) purified with 1.2x volumes of SPRI beads. Library preparation for high-throughput sequencing: The aRNA was chemically fragmented into short molecules (median size ~200 nucleotides) by incubating 3 min at 70°C in Zn^{2+} RNA fragmentation solution (Ambion) and purified with two volumes of SPRI beads. The aRNA (5 μl) was pre-incubated 3 min at 70°C with 1 μl of 100 μM ligation adaptor; then, 14 μl of a mix containing 9.5% DMSO, 1 mM ATP, 20% PEG8000 and 1 U/μl T4 ligase in 50 mM Tris HCl pH7.5, 10 mM $MgCl_2$ and 1mM DTT was added. The reaction was incubated at 22°C for 2 hr. The ligated product was reverse transcribed using Affinity Script RT enzyme (Agilent; reaction mix contains Affinity Script RT buffer, 10 mM DTT, 4 mM dNTP, 2.5 U/μl RT enzyme) and a primer complementary to the ligated adaptor. The reaction was incubated for 2 min at 42°C, 45 min at 50°C and 5 min at 85°C. The cDNA was purified with 1.5x volumes of SPRI beads. The library was completed and amplified through a nested PCR reaction with 0.5 μM of P5_Rd1 and P7_Rd2 primers and PCR ready mix (Kapa Biosystems). The forward primer contains the Illumina P5-Read1 sequences and the reverse primer contains the P7-Read2 sequences. The amplified pooled library was purified with 0.7x volumes of SPRI beads to remove primer leftovers. Library concentration was measured with a Qubit fluorometer (Life Technologies) and mean molecule size was determined with a 2200 TapeStation instrument (Agilent). MARS-Seq libraries were sequenced using an Illumina HiSeq 1500.

Processing and Analysis of RNA-Seq Data

We sequenced an average of 4 million reads per library. All reads were aligned to the mouse reference genome (NCBI 37, mm9) using the TopHat aligner (Trapnell et al., 2009) with default parameters. The raw expression levels of the genes were calculated using ESAT (http://garberlab.umassmed.edu/software/esat).

Briefly, ESAT is a new methodology implemented specifically for the analysis of digital expression RNA-Seq libraries described in our previous work (Garber et al., 2012). ESAT takes as input a transcriptome annotation set (we used RefSeq annotations

downloaded from the UCSC genome browser), and uses a scanning window approach to assign the most enriched peak to each annotation. This is done for every isoform, and the ends are collapsed for the genes. We use the collapsed gene counts for our analysis. Based on the principles of the protocol, raw read counts can be used directly for gene expression, as gene length bias is eliminated when sequencing fixed-length fragments at the gene end. Multiple samples are processed together by ESAT by assignment of the region most covered in all samples. When processing multiple samples, ESAT identified the region most covered across all samples and assigns for each gene in each sample the number of reads that aligned to this region. Multi-mapped reads are downweighed by the number of mappings. Counts are rounded to the nearest integer and normalized using a method previously described (Anders and Huber, 2010). For every gene we compute the geometric mean across samples. The normalization constant for each sample is computed as the median gene fold change over this geometric mean. This normalization method is robust against not only difference in sequencing depth but also to variations in the RNA composition.

To generate the heatmap of K-mean clusters, we used GENE-E (http://www.broadinstitute.org/cancer/software/GENE-E/) set to global comparison and average-centered. K was chosen at 11 because lower values failed to identify all meaningful clusters and higher values subdivided meaningful clusters. In populations with more than 2 replicates, we chose to display the pair with the greatest correlation. Low expression values were set equal to the 25th percentile.

ATAC-Seq

To profile for open chromatin, we used the Assay for Transposase Accessible Chromatin (ATAC-seq) protocol developed by (Buenrostro et al., 2013). The following modifications were added: macrophage subpopulations were sorted in 400ul of MACS buffer (1x PBS, 0.5% BSA, 2mM EDTA) and pelleted by centrifugation for 15min at 500 g and 4°C using a swing rotor with low acceleration and brake settings. Cell pellets were washed once with 1x PBS and cells were pelleted by centrifugation using the previous settings. Cell pellets were re-suspended in 25ul of lysis buffer (10mM Tris-HCl pH 7.4, 10mM NaCl, 3mM $MgCl_2$, 0.1% or 0.5% Igepal CA-630) and nuclei were pelleted by centrifugation for 30min at 500 g, 4°C using a swing rotor with low acceleration and brake settings. Supernatant was discarded and nuclei were re-suspended in 25 μl reaction buffer containing 2ul of Tn5 transposase and 12.5ul of TD buffer (Nextera Sample preparation kit from Illumina). The reaction was incubated at 37°C for one hour. Then 5ul of clean up buffer (900mM NaCl, 300mM EDTA), 2ul of 5% SDS and 2ul of Proteinase K (NEB) were added and incubated for 30min at 40°C. Tagmentated DNA was isolated using 2x SPRI beads cleanup. For library amplification, two sequential 9-cycle PCR were performed in order to enrich small tagmentated DNA fragments. We used 2ul of indexing primers included in the Nextera Index kit and KAPA HiFi HotStart ready mix. After the first PCR, the libraries were selected for small fragments (less than 600 bp) using SPRI cleanup. Then a second PCR was performed with the same conditions in order to obtain the final library. DNA concentration was measured with a Qubit fluorometer (Life Technologies) and library sizes were determined using TapeStation (Agilent Technologies). Libraries where sequenced on a Hiseq 1500 for an average of 5 million unique reads per sample.

High-Throughput-ChIP-Seq

In brief, following cross-linking and sorting, cells were lysed for 10 min on ice in RIPA buffer supplemented with protease inhibitors (Roche), and then chromatin was fragmented by sonication for 4.5 min at 45% amplitude (Branson Digital Sonifier, Branson Ultrasonics). Sonicated material was cleared by a 10 min centrifugation at 4°c. Immunoprecipitation was performed by mixing the cleared sonicated material with 50ul of magnetic protein G beads (Invitrogen, Dynabeads) conjugated to 1ng of either H3K4Me1 (Abcam and Millipore), H3K4Me2 (Abcam), H3K4Me3 (Millipore) or H3K27Ac (Abcam) antibodies, and tumbling for 4 hr at 4°c. Unbound lysate was then removed, and beads excessively washed with ice-cold RIPA, high-salt RIPA, LiCl and TE buffers. Chromatin was eluted from the beads, then treated with RNase (Roche) for 30 min at 37°c and with Proteinase K (NEB) for 2 hr at 37°c. Reverse cross-linking was performed at 65°c overnight. DNA was purified with SPRI beads (Agencourt AMPure XP beads, Beckman Coulter) at 2.3x ratio. Sequential steps of end-repair, A-base addition, adaptor-ligation and amplification were performed, with DNA purification with SPRI beads after each step. Following the amplification step, DNA concentration was measured, and equivalent amounts of barcoded ChIPed DNA from each sample were pooled together. An additional size-selection step was performed, and pooled DNA was sequenced (HiSeq 1500, Illumina) with an average of 10^7 reads per sample. For input DNA to be used as control for background noise, we fragmented 1ng of chromatin for each sample, which underwent all steps of the ChIP-seq protocol except for immunoprecipitation and washing.

Chromatin Details by Figure

We limited our chromatin analysis to high confidence regions where the read density of both replicates were within the top 25th percentile and > 2-fold over the density of input reads (background). This cutoff matches the RNA-seq analysis and the resulting regions reflected the higher end of enriched signal after the peaks were merged across cell types into the union file. For H3K4me3, these regions were highly enriched for annotated promoters (Data S1). The threshold over background eliminated multiple regions that suffered from clonal bias while preserving the H3K4me1 regions with signal extended over a large area.

For the Venn diagrams in Figure 2, regions were classified as shared if the intensity (minimum for macrophages) of the region was < 2-fold higher than the intensity (maximum for macrophages) of the other cell type(s). Similarly, for the related supplement (Figure S2), we considered a region shared between *x* populations if the difference between the maximum and minimum intensities in these populations is < 2-fold.

For the correlation heatmaps such as Figure 4A, we calculated the pairwise Pearson's correlation between samples (and replicates) using the H3K4me1 read density. Similar figures for each assay appear in the supplement. For Figure 5B and other cross-assay heatmaps, we calculated the pairwise Pearson's correlations between the intensity of the two assay in all samples.

For the clustering of enhancers in Figure 4B, we used the matlab K-means algorithm with the Euclidean distance metric. K was chosen at 20 because lower values failed to identify all meaningful clusters and higher values subdivided existing clusters. Enhancers were associated to the nearest gene within 50 kb with intragenic annotations taking precedent over intergenic. We set the threshold for H3K27ac read density in enhancer activity at 15 in any cell type before normalization. At this value, the most active enhancers were included with the number comparable across populations at around 40% overall (Data S1). Changes to the threshold did not affect the relative proportion of active enhancers between clusters. In the follow-up analysis of Figure 4E, we avoided the threshold issue altogether by displaying the average H3K27ac intensity.

Hierarchical clustering based on intensity of H3K4me1 (Figure 4C), H3K4me2 (Figure S3), or H3K27ac (Figure S4) in enhancers was performed using Pearson's correlation distance metric.

In Figure 4D, we considered a monocyte enhancer shared if the difference between the intensity in the given tissue-resident macrophage was < 2-fold.

Motif Finding in ATAC-Seq Peaks

To confirm the association between H3K4me1 and ATAC-seq, we calculated the ATAC-seq intensity in H3K4me1-marked enhancers (as described above, Figure S6). We overlapped the ATAC-seq union peaks file with the enhancer regions and extracted the sequence of the maximum overlapping peak. We used the known motif results to find which of the motifs in the HOMER database were enriched in our data sets according to HOMER ($p \leq 10^{-5}$; exact values are shown in Table S4). For the motif analysis comparing myeloid cell types in Figures 2C and 2D, we compared 500 bp sequences centered on the ATAC-peak in cell-type-specific H3K4me1-marked region to the remaining enhancers as background. For the motif analysis of H3K4me1 clusters in Figure 5D, we used a random set of background regions as chosen by HOMER. Exact locations of motifs were determined by IGV motif finder algorithm (Robinson et al., 2011).

Bone Marrow Transplant Analysis

We calculated the density of transplant reads in the original enhancer regions from the reference macrophages. We also called peaks in the transplant cells as described above. Then, we identified novel H3K4me1-marked regions in the transplant union peaks file that did not overlap regions from the reference macrophages. We added these novel regions to the original regions to identify which were the high confidence regions with densities in the top 25th percentile and 2-fold greater than the input. We removed regions on chrX from this analysis to avoid artifacts from the mis-alignment of chrY (donor mice were male but recipient mice were female). Then, we determined the density of H3K4me1 reads from reference macrophages in the novel regions. To compare the transplant cells to the reference macrophages, we calculated the intensities of H3K4me1 and H3K27ac for transplant cells and reference macrophages in all regions (novel and original). For Figures 6E and S6H, we classified original enhancers as recovered in transplant cells, if the intensity was less than 2-fold different. Finally, PCA was performed on the vector of these intensities across all regions using the matlab algorithm *pca*.

Transfer Analysis

For Figures 7E and 7F, lung, peritoneal, and transferred macrophages were sorted or analyzed from mice in the same experiment with control (PBS) or transferred macrophages. Values are representative of two replicate experiments. For Figures 7G and 7H, we compared expression of transferred cells to reference peritoneal or lung macrophages from Figure 1. The heatmap is based on genes expressed over 100 a.u. in at least one of the reference macrophages with a 2-fold difference between them. Expression is represented in log2 scale and low expression values were set equal to the 25th percentile. The rows were sorted by whether the gene expression was higher in lung or peritoneal macrophages and whether the transferred expression resembled the lung macrophage signature (i.e., if the difference between the average expression of transferred cell was closer to lung than peritoneal macrophages). PCA was done on the slightly less stringent set of the top 1,600 expressed genes using the matlab algorithm *pca*.

Comparison to Stimulated Cells

The stimulation data included microarray expression for dendritic cells (DCs) under 4 time points of LPS stimulation and control (Garber et al., 2012). We extracted expression values for all genes that were found in both data sets. Then, we calculated the pairwise Pearson's correlation between our tissue-resident macrophage populations and each time point.

Conservation

We downloaded the phyloP conservation scores for placental mammals from the UCSC browser (Pollard et al., 2010). We extracted the maximum value for each enhancer region as it conservation score.

K4me2 Confirmation

We calculated H3K4me2 intensity in H3K4me1-marked regions as described above to corroborate our definition of enhancers in the cell types for which it was available (Figure S5).

GO Annotation Analysis

For expression data, GO annotation was determined using the Gorilla tool on each of the 11 clusters in Figure 1B (Eden et al., 2009). For enhancers, enriched MSigDB Pathways were compiled from the GREAT tool (McLean et al., 2010) on each of the 20 enhancer clusters in Figure 4B. In both cases, pathways were ranked using p-value or binomial raw p-value respectively.

SUPPLEMENTAL REFERENCES

Anders, S., and Huber, W. (2010). Differential expression analysis for sequence count data. Genome Biol. *11*, R106.

Eden, E., Navon, R., Steinfeld, I., Lipson, D., and Yakhini, Z. (2009). GOrilla: a tool for discovery and visualization of enriched GO terms in ranked gene lists. BMC Bioinformatics *10*, 48.

McLean, C.Y., Bristor, D., Hiller, M., Clarke, S.L., Schaar, B.T., Lowe, C.B., Wenger, A.M., and Bejerano, G. (2010). GREAT improves functional interpretation of cis-regulatory regions. Nat. Biotechnol. *28*, 495–501.

Pollard, K.S., Hubisz, M.J., Rosenbloom, K.R., and Siepel, A. (2010). Detection of nonneutral substitution rates on mammalian phylogenies. Genome Res. *20*, 110–121.

Robinson, J.T., Thorvaldsdóttir, H., Winckler, W., Guttman, M., Lander, E.S., Getz, G., and Mesirov, J.P. (2011). Integrative genomics viewer. Nat. Biotechnol. *29*, 24–26.

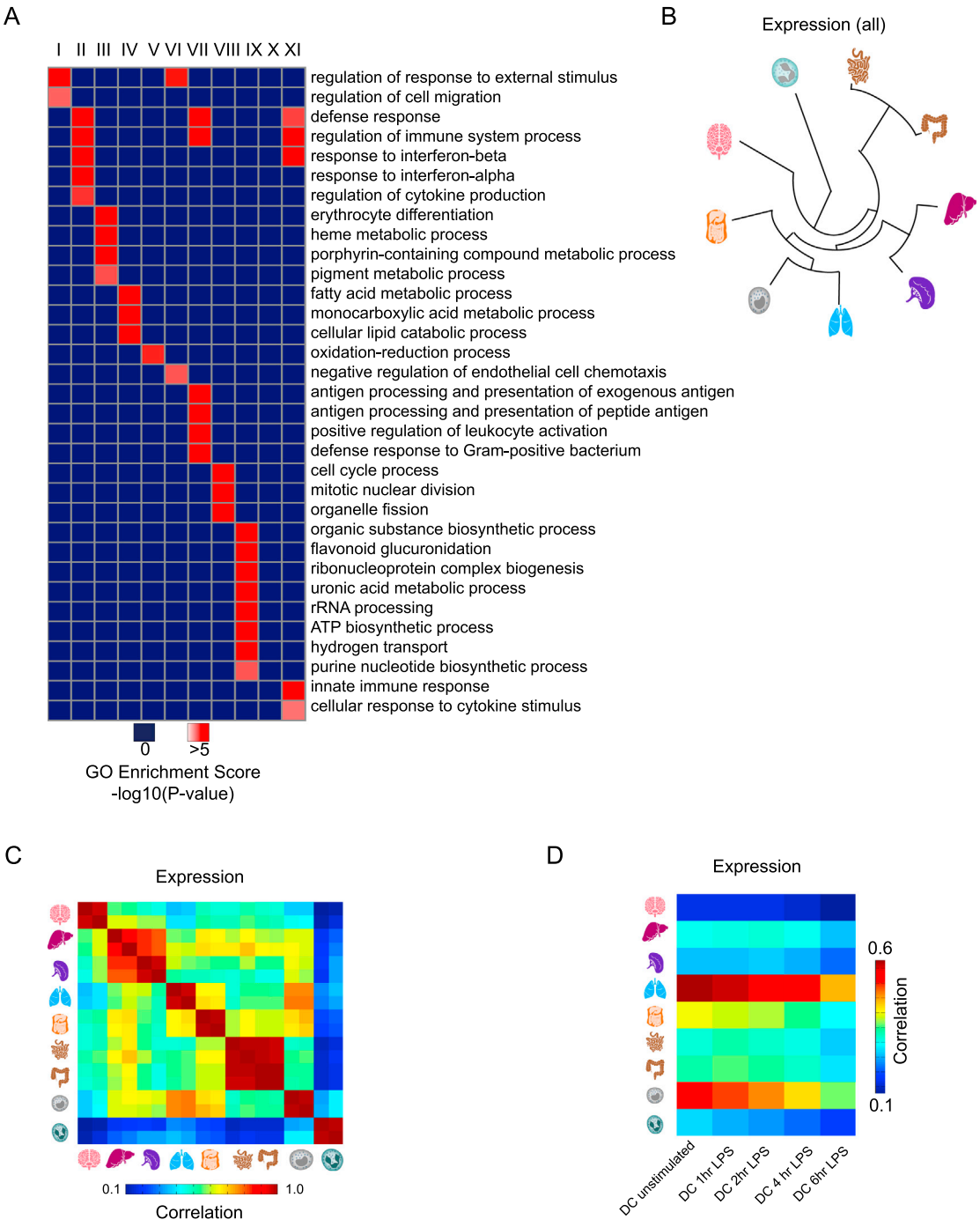

Figure S1. Tissue-Resident Macrophages Exhibit Diverse Gene Expression Signatures Associated with Distinct Pathways, Related to Figure 1

(A) GO annotation pathways for each of 11 clusters in Figure 1B (red indicates $p < 10^{-5}$).

(B) The hierarchical tree resulting from clustering macrophages, monocytes, and neutrophils on average of replicates in each population based on all expression data.

(C) Pairwise correlations between all samples with respect to expression.

(D) Pairwise correlations between macrophages, monocytes, and neutrophils in the current study versus LPS stimulation time points of dendritic cells from (Garber et al., 2012) with respect to expression of all genes. Our samples are most correlated to unstimulated cells (t0).

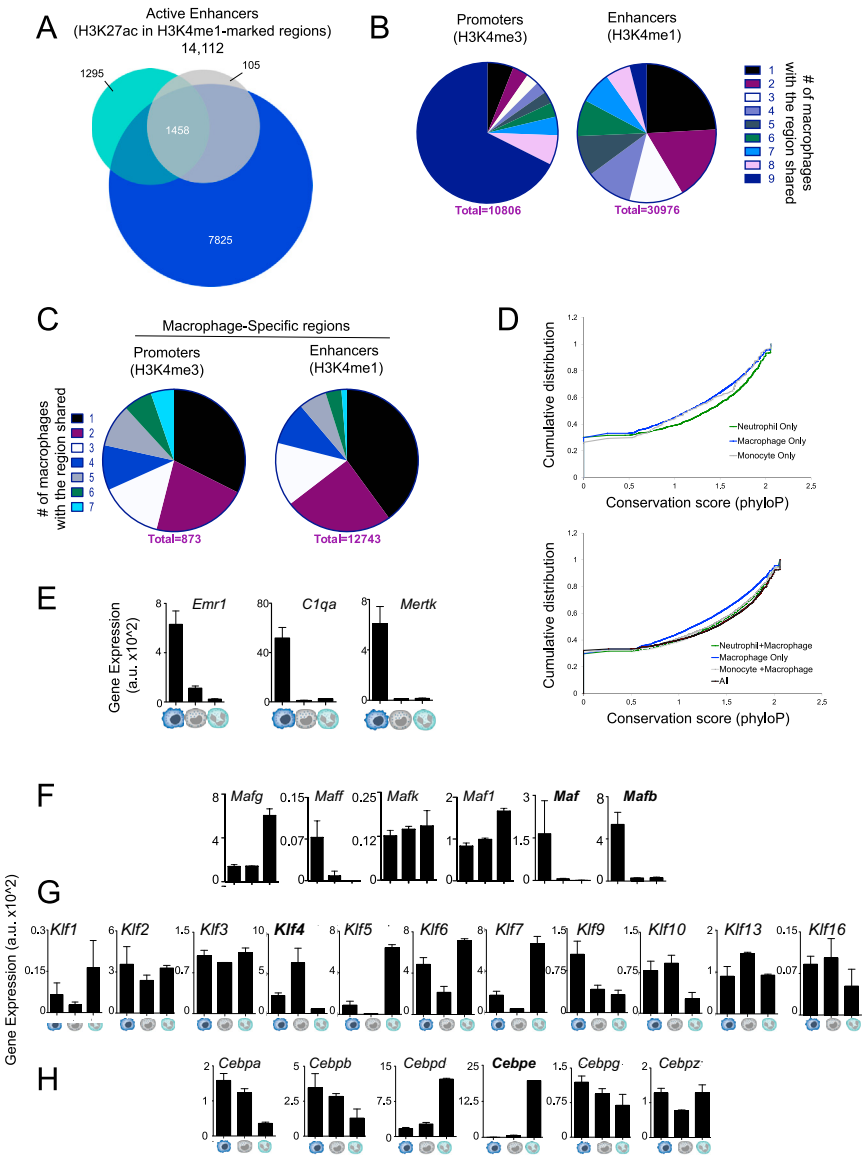

Figure S2. Myeloid Cells Have Distinct Chromatin Landscapes and Conservation, Related to Figure 2

(A) Venn diagrams representing the overlap of active enhancers (14,112) between macrophages, monocytes, and neutrophils. Macrophage enhancers were required to be active in at least one of the seven tissue-resident macrophages.

(B) Pie chart of all promoters (left) and enhancers (right) indicating the number of samples (including monocytes and neutrophils) in which the region is shared (1-9). The number of unique regions is greater in enhancers than promoters (1, black).

(C) Pie chart of macrophage-specific promoters (left) and enhancers (right) indicating the number of macrophage populations in which the region is shared (1-7). The number of regions shared by all macrophage populations (7, light blue) is smaller in enhancers than promoters.

(D) Cumulative distribution function (cdf) of conservation scores (phyloP) in enhancers for macrophage-specific, monocyte-specific, or neutrophil-specific H3K4me1-marked regions (top) and macrophage-specific, macrophage/monocyte-shared, macrophage/neutrophil-shared, or all-shared H3K4me1-marked regions (bottom). In either case, the macrophage-specific regions (blue) are the least conserved ($p < 10^{-10}$, except compared to monocyte-specific).

(E) Bar graphs of expression in monocyte, neutrophils, and average of all macrophage populations corresponding to the genes within the loci shown in Figure 2B – represented in arbitrary units (a.u.).

(F–H) Bar graphs of gene expression (a.u.), for members of the (F) MAF, (G) KLF, and (H) CEBP families of transcription factors in monocytes, neutrophils, and the average of all macrophage populations. The bold genes correspond to those chosen for Figure 2D because they match the motif occurrence across cell types. Error bars indicate SEM.

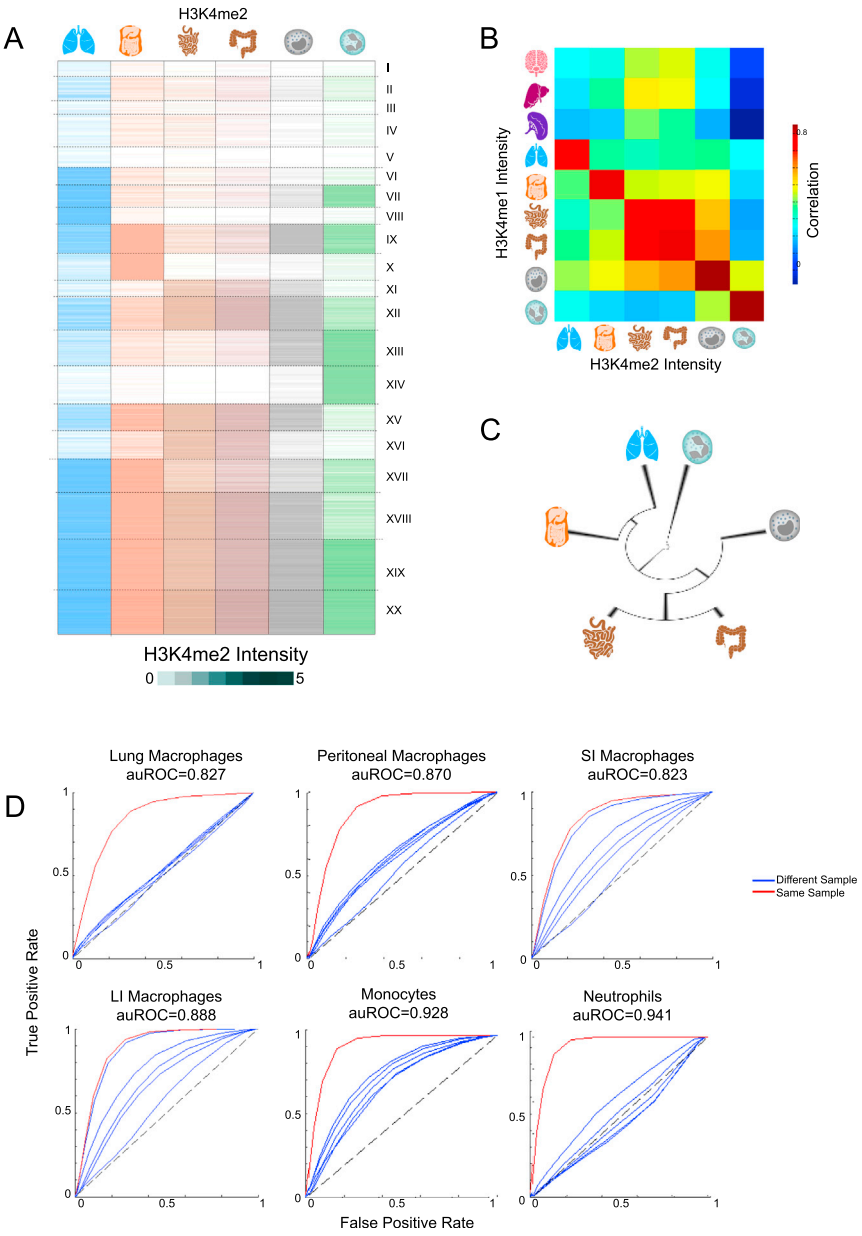

Figure S3. H3K4me2 Also Marks Enhancers and Validates H3K4me1-Marked Regions, Related to Figure 4

(A) H3K4me2 intensity in enhancer regions as clustered in Figure 4B.

(B) Pairwise correlations between H3K4me2 and H3K4me1 intensity in enhancers for macrophages, monocytes, and neutrophils.

(C) The hierarchical tree resulting from clustering of all macrophages, monocytes, and neutrophils based on H3K4me2 intensity in enhancer regions.

(D) ROC curve for the prediction of H3K4me1-marked regions by H3K4me2 intensity. Red line indicates the curve for the prediction within the same sample whereas blue lines indicate the curves for prediction of regions in different samples. Value for area under the ROC curve (auROC) is indicated for the red line (perfect prediction auROC = 1, random prediction auROC = 0.5 indicated by black dashed line).

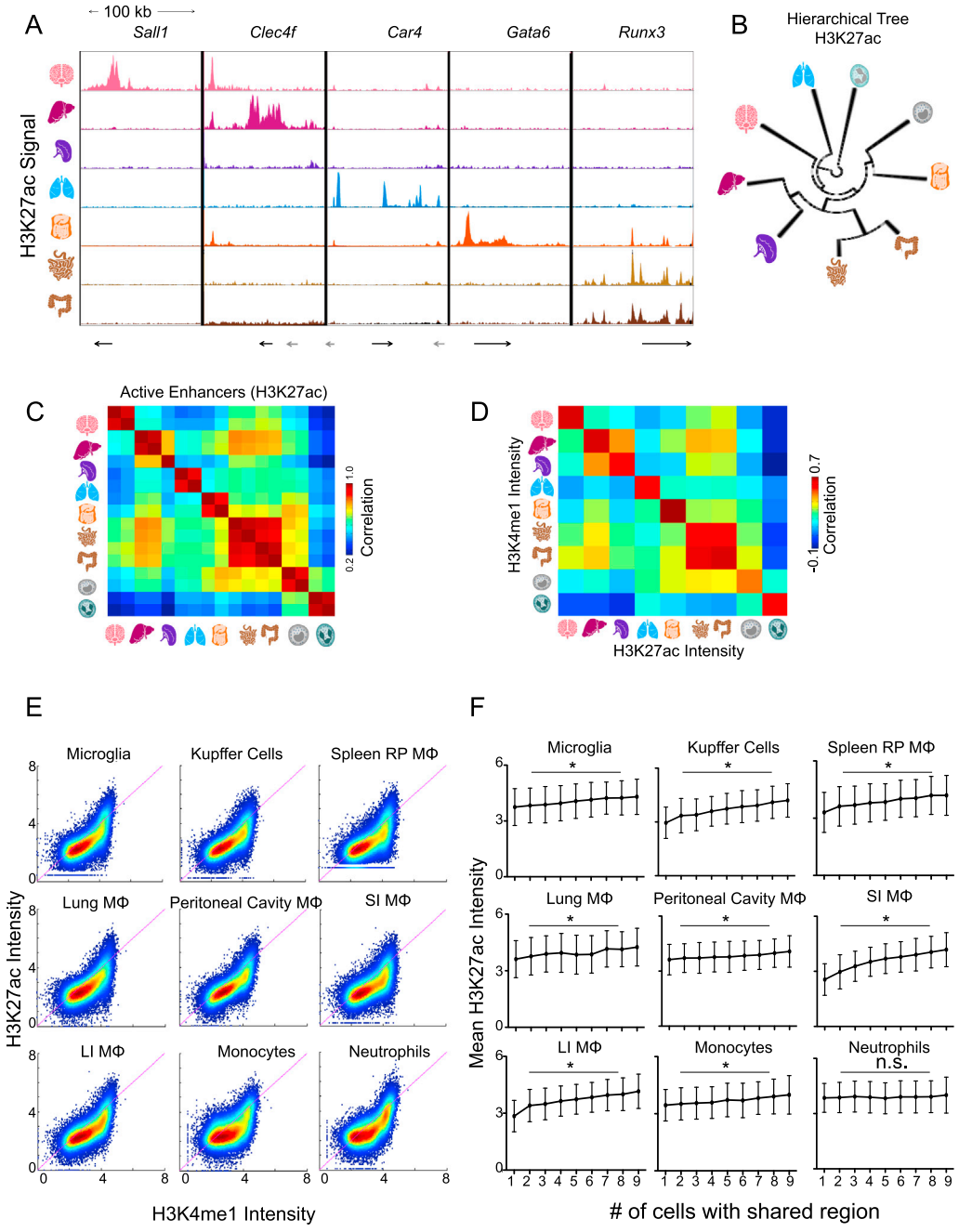

Figure S4. Activity Level of Enhancers Measured by H3K27ac Distribution in Tissue-Resident Macrophages, Related to Figure 4

(A) Normalized profiles of H3K27ac signal of seven tissue-resident macrophage populations in 100 kb regions containing the tissue-specific enhancers around indicated genes from Figure 3A.

(B) The hierarchical tree resulting from clustering of all macrophages, monocytes, and neutrophils based on H3K27ac intensity in enhancer regions.

(C) Pairwise correlations between all samples with respect to H3K27ac read density for replicates in enhancer regions.

(D) Pairwise correlations between H3K4me1 and H3K27ac intensity in enhancer regions for macrophages, monocytes, and neutrophils.

(E) Density scatter plots comparing H3K27ac and H3K4me1 intensity for each sample in all enhancer regions. Regions with high H3K4me1 and H3K27ac are considered active enhancers while regions with high H3K4me1 and low H3K27ac are considered poised enhancers. Pink line indicates where H3K4me1 and H3K27ac intensity are equal.

(F) Line graphs showing that enhancer activity level (mean H3K27ac intensity) increases with the number of samples that share the H3K4me1-marked regions (error bars show standard deviation; * indicates significant difference between 2 and 8, t test $p < 10^{-5}$).

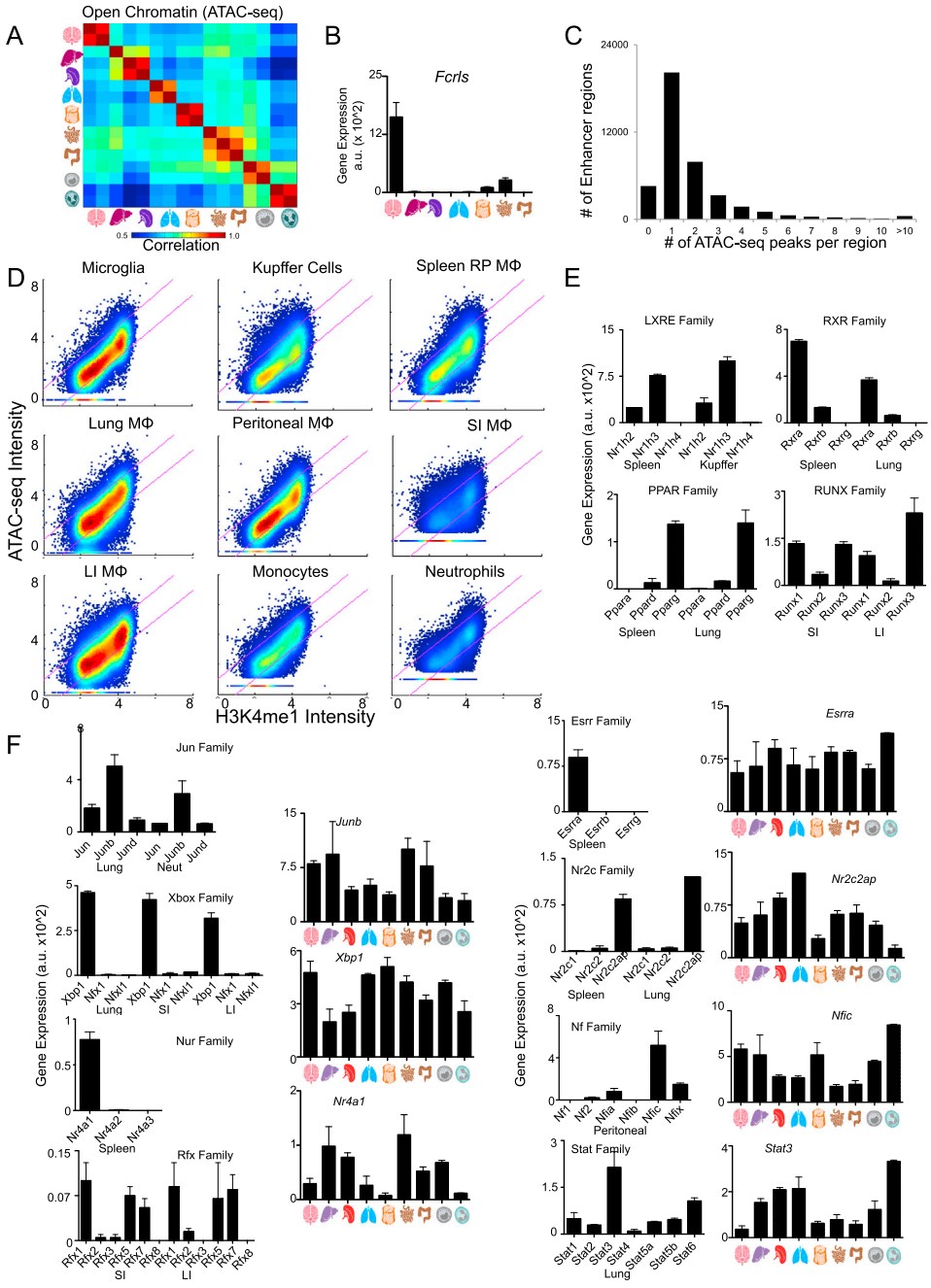

Figure S5. TF Motifs in ATAC-Seq Peaks and Expression Levels Are Used to Implicate Regulators of Tissue-Resident Macrophages, Related to Figure 5

(A) Pairwise correlations between all samples with respect to ATAC-seq read density for replicates in enhancer regions.

(B) Bar graph of gene expression (a.u.) for *Fcrls* whose gene locus is shown in Figure 5C. Error bars indicate SEM.

(C) Histogram of the number of ATAC-seq peaks found in enhancer regions.

(D) Density scatter plots comparing ATAC-seq and H3K4me1 intensity for each sample in all enhancer regions. Pink lines indicate regions of 2-fold change or more.

(E) Bar graphs of gene expression (a.u.) for members of the transcription factor families shown in Figure 5E (but not 5C) in the macrophage populations of interest. Error bars indicate SEM.

(F) Bar graphs of gene expression (a.u.) for members of the transcription factor families shown in Figure 5D (but not 5E) in the macrophage populations of interest. Gene expression (a.u.) across all populations is shown for the family member with the highest relevant expression. Error bars indicate SEM.

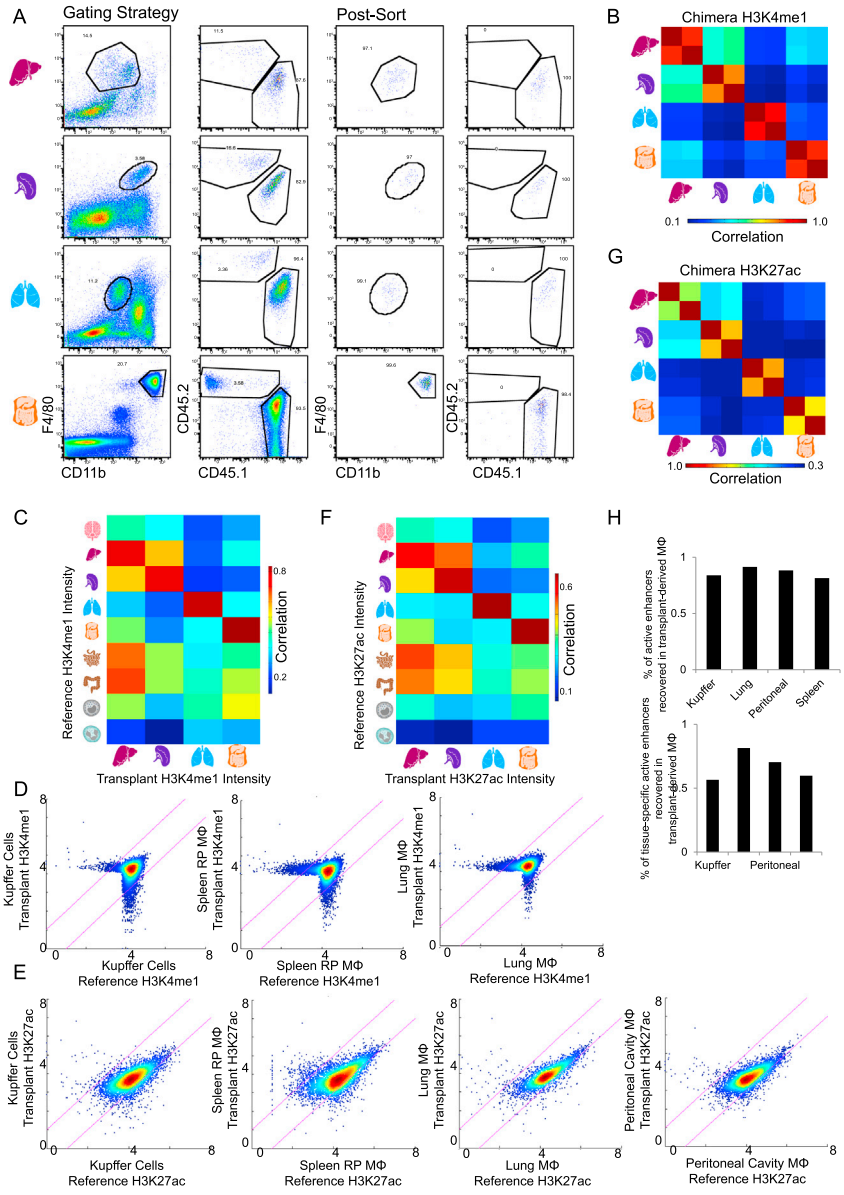

Figure S6. Transplanted Macrophages Recapitulate the Enhancers of Their Respective Embryo-Derived Counterparts in H3K4me1 and H3K27ac Intensity, Related to Figure 6

(A) FAC plots showing gating strategy for sorting transplanted macrophages based on CD45.2 (host) and CD45.1 (transplant). Post-sort analysis of cross-linked transplant macrophages is shown (right).

(B) Pairwise correlations between transplanted macrophage populations with respect to H3K4me1 read density for replicates in original and novel enhancers.

(C) Pairwise correlations between transplanted macrophage and all reference macrophage populations with respect to H3K4me1 intensity in original and novel enhancers (see methods).

(D) Density scatter plots of H3K4me1 intensity for reference (x axis) and transplant-derived (y axis) tissue-resident macrophages in original and novel enhancers. Pink lines indicate regions of 2-fold change or more.

(E) Density scatter plots of H3K27ac intensity for reference (x axis) and transplant-derived (y axis) tissue-resident macrophages in original and novel enhancers. Pink lines indicate regions of 2-fold change or more.

(F) Pairwise correlations between transplanted macrophage and all reference macrophage populations with respect to H3K27ac intensity in original and novel enhancers.

(G) Pairwise correlations between transplanted macrophage populations with respect to H3K27ac read density for replicates in original and novel enhancers.

(H) Bar graph showing the percent of total (left) or tissue-specific (right) active H3K4me1-marked enhancers from reference macrophages that recovered H3K27ac intensity in transplant-derived macrophages.

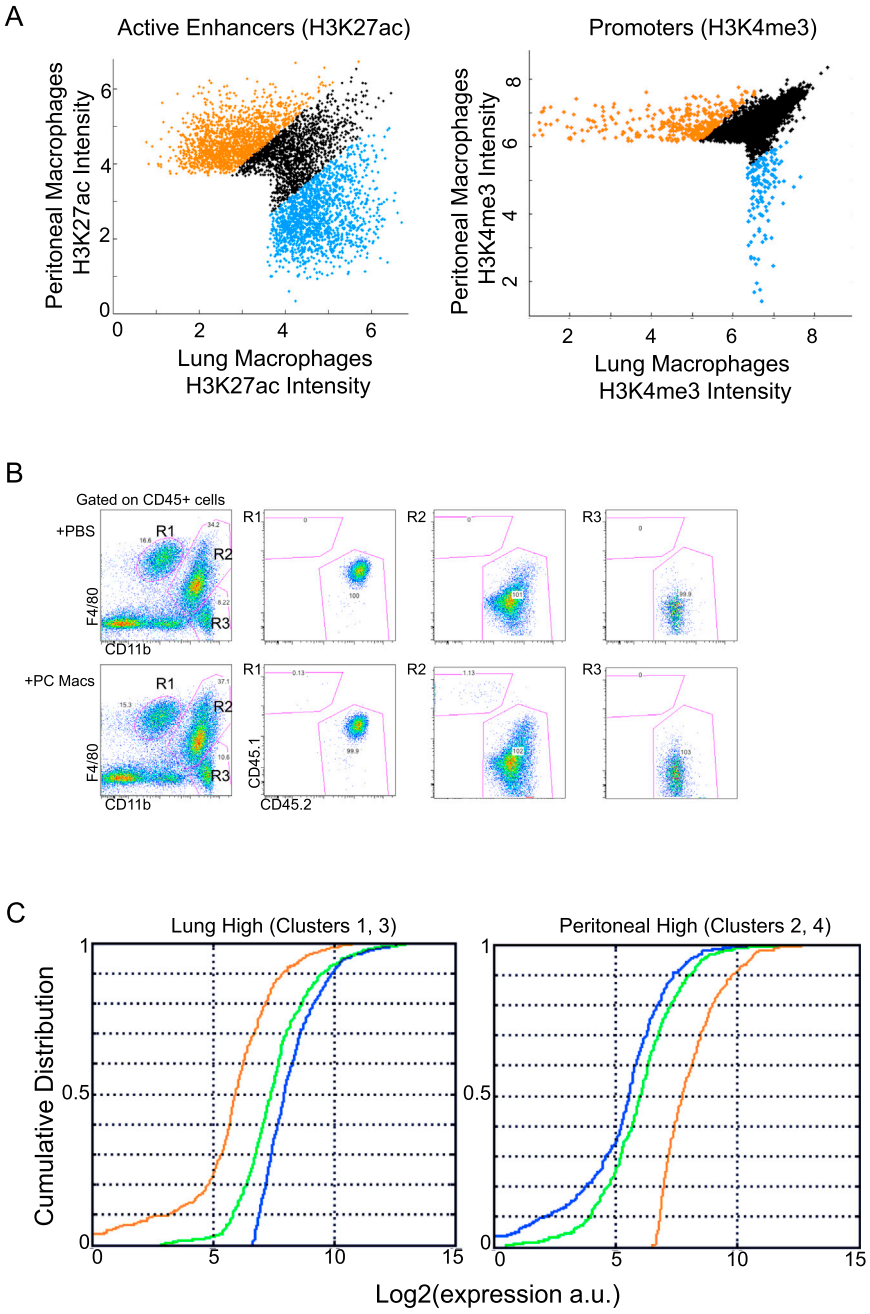

Figure S7. Peritoneal and Lung Macrophages Have Distinct Regulatory Networks, Related to Figure 7

(A) Scatter plots comparing H3K27ac intensity in peritoneal cavity and lung macrophage active H3K4me1-marked regions (left) and H3K4me3 intensity in peritoneal cavity and lung macrophage promoters (right). Differential regions (2-fold change) in peritoneal cavity (orange) and lung (blue) macrophages are indicated.

(B) FACs plots showing lung CD45+ populations with PBS or peritoneal cavity macrophages transplanted intratracheally. Transplanted macrophages, identified by CD45.1, appear in R2, where they retained high CD11b expression and some in R1 where they appear to be downregulating the integrin, similar to lung macrophages.

(C) Cumulative distribution functions (cdfs) of peritoneal cavity (orange), lung (blue) and transplant (green) macrophage expression in genes that are highly and differentially expressed in lung (left) and peritoneal cavity (right) macrophages. Transplant expression is closer to the lung macrophage expression signature and significantly different (kstest $p < 10^{-5}$) from that of the peritoneal cavity.